A Model for Mesh Stiffness Evaluation of Spur Gear with Tooth Surface Wear

Xiuquan Sun, Tie Wang, Ruiliang Zhang, Fengshou Gu, Andrew D. Ball

A Model for Mesh Stiffness Evaluation of Spur Gear with Tooth Surface Wear

Xiuquan Sun[1, 2], Tie Wang[1], Ruiliang Zhang[1], Fengshou Gu[2,*], Andrew D. Ball[2]

[1]Taiyuan University of Technology, School of Mechanical Engineering, Taiyuan, 030024, China
[2]University of Huddersfield, CEPE, School of computing and Engineering, Huddersfield, HD1 3DH, UK
xiuquan.sun@hud.ac.uk, wangtie57@163.com, f.gu@hud.ac.uk, rl_zhang@163.com, a.ball@hud.ac.uk

Abstract

Gear tooth wear commonly exists on the mating tooth surfaces under the harsh conditions like long-time operation and inadequate lubrication. However, detecting the wear is a challenging task for researchers due to the complicated contact state and limited effect on gear dynamics. Despite a number of studies have been conducted recently on the gear wear process numerically and experimentally, the understanding of gear wear mechanism is still limited due to the complicated coupling working conditions between the mating teeth, such as lubrication regime, heating effect, time-varying friction and the changes in load and speed. Normally, the accumulated tooth wear can lead to the deviation of gear tooth profile which will cause the change in gear mesh stiffness. Furthermore, it will result in the deterioration of gear dynamics. This study proposed a modified model for predicting the gear mesh stiffness with various tooth surface wear severities. In this model, the Hertzian contact theory and Archard's wear equation were employed to calculate the wear depth which further was substituted into the involute gear profile equation. Furthermore, the model of the modified time-varying mesh stiffness (TVMS) was then derived by employing the potential energy method with the updated gear tooth profile. This modified TVMS model was applied onto a spur gear set, and the results illustrate that the tooth wear will cause a reduction in gear tooth mesh stiffness.

1   Introduction

Gear tooth wear is usually understood as a process of progressive material removal on the mating tooth surfaces which mainly results from the inadequate lubrication and extreme working conditions. The wear may cause some negative effects on gear transmission system such as non-uniform gear rate, poor dynamic behaviour and potential severe gear failures. Moreover, in high precision machining field, the gear tooth wear may affect the accuracy and quality of machining products and further cause great economic loss.

As addressed in many studies, gear tooth wear and gear dynamics are mutually affected by each other. The tooth surface wear can result in the deterioration in the gear tooth profile and alter the gear mesh excitations, which further will influence the dynamic behaviour of a gear transmission system. Theories of progressive wear have been investigated for decades and lots of papers were published based on different wear models.

Flodin and Andersson [1-2] simulated the mild wear of spur gear by substituting the contact parameters derived from a Winkler surface model into the Archard's wear model. Afterwards, they simulated the helical gear wear by equivalising the helical gear as a combination of numbers of slices of spur gear [3-4]. K. Mao use finite element method to simulate gear contact behaviour considering the effect induced by shaft misalignment, deflection and assembly deflection. Kahraman [5] investigated the influence of tooth profile deviation on helical gear wear and found that the wear is related to the combined modification parameters rather than individual gear parameters. Mert [6] theoretically and experimentally investigated the wear in internal gears with different torques and motor speeds by adopting Archard's wear equation. Valentin [7] investigated the tooth wear from scuffing of heavy duty machine spur gears taking the the instantaneous contact

temperature into account. Some other studies[8-10] also had been carried out to predict gear tooth wear, however, the influence of tooth wear on gear contact parameters are not investigated extensively.

This study proposed a modified model for determining the time-varying mesh stiffness under different gear tooth wear severities and various loads conditions. The Hertzian contact theory was employed to derive the contact pressure and contact width. Then the wear depth was estimated by substituting the time-varying sliding distance and contact pressure into the Archard's wear equation. By integrating the gear wear depth with the involute gear tooth profile, the time-varying gear mesh stiffness can be determined using the potential energy method. The following sections will illustrates the modelling process in detail.

2   Gear wear model

2.1   Gear meshing process

With the movement of the meshing point on the gear involute profile, the radius of the meshing point on the driving gear will increase gradually. Conversely, the radius of the meshing point on the driven pinion will decrease gradually. According to the position of the meshing point, the motion of the meshing point can be divided into three cases: the first case is when the meshing point is before the pitch point; the second one is when the meshing point coincides with the pitch point; the third one is when the meshing point is after the pitch point. For the first case, the radius of the meshing point on the gear is smaller than that on the pitch circle, meanwhile, the radius of the meshing point on the pinion is larger than that on the pitch circle. Correspondingly, this variation in radius will cause that the velocity of the meshing point on the gear is lower than that on the pinion. Furthermore, the relative sliding motion between gear and pinion are generated. Figure 1 (a) shows the direction of the friction induced by the sliding motion under the first case. With the movement of the meshing point on the gear profile, when the meshing point coincide with the pitch point, the linear velocity of the gear at the meshing point equals to that of the pinion, there is no relative sliding motion at this moment, only rolling motion as shown in Figure 1 (b). However, for the third case, when the meshing point passes through the pitch point, the direction of the friction will be opposite compared to that in the first case as shown in Figure 1 (c), which is resulted from the change in the velocity of gear and pinion.
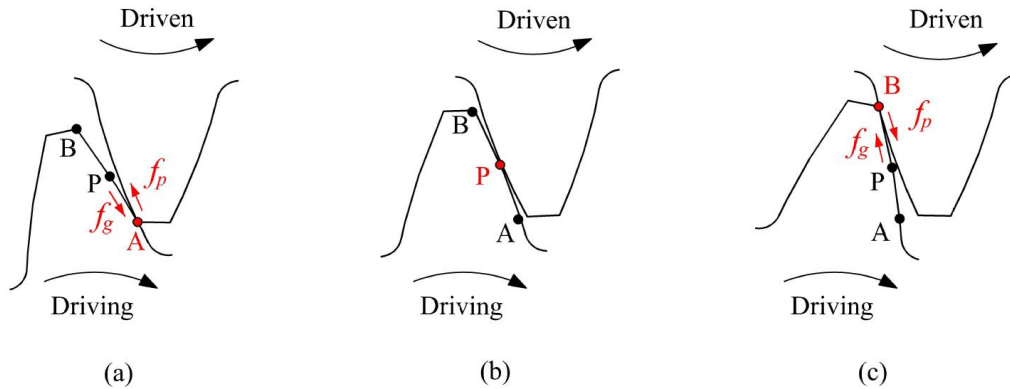

Figure 1 The change in sliding motion in one tooth mesh process

As described above, the sliding motion and rolling motion along the line of action is time-varying. It is very necessary to consider this time-varying characteristic when doing the modelling of gear wear process.

2.2   Hertzian contact theory

According to the Hertzian contact theory, the gear tooth contact can be treated as the contact of two cylinders with parallel axes. The semi-Hertzian contact width can be obtained as:

$$a_h = \sqrt{\frac{4F_t \rho}{\pi b E}} \tag{1}$$

where F_t is the tangential force, ρ is the equivalent curvature radius of the contacting surfaces, $\frac{1}{\rho} = \frac{1}{\rho_1} - \frac{1}{\rho_2}$, E is the equivalent elasticity modulus of materials, $\frac{1}{E} = \frac{1-v_1^2}{E_1} + \frac{1-v_2^2}{E_2}$, b is the gear width.

The maximum contact pressure along the centre line of the rectangular contact area is:

$$P_{max} = \frac{2F_t}{\pi a_h b} \tag{2}$$

2.3 Sliding distance

When a pair of meshing points come into mesh, they have three relative positions in the contact region. As shown in Figure 2 (a), at the beginning of the meshing process, the two points are coincided with each other and there is no sliding distance between the two points. However, with the movement of the meshing points, the sliding distance will increase continuously under the influence of different peripheral velocities. When the point P_p on the pinion firstly moves to the edge of the contact region while the P_g is still in the contact region, the sliding distance S_{p1} corresponding to the pinion arises between the two points as shown in Figure 2 (b). At the third position, a distance S_{p2} corresponding to the gear arises when the point P_g is about to leave the contact region.
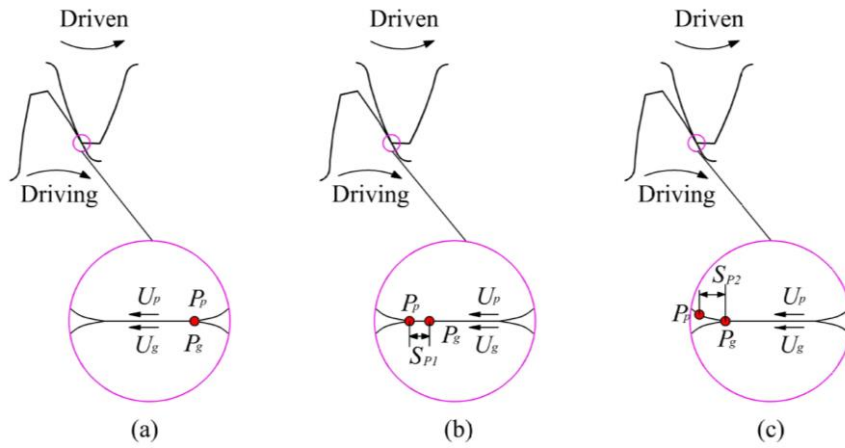

Figure 2 The relative sliding distance between the meshing points on gear and pinion

The sliding distances between the points for gear and pinion can be calculated as:

$$S_{p1} = 2a_h \frac{U_p - U_g}{U_p} \tag{3}$$

$$S_{p2} = 2a_h \frac{U_g - U_p}{U_g} \tag{4}$$

where α_h is the semi-Hertzian contact width which can be obtained from the Eq (1), U_g and U_p are the peripheral velocities of gear and pinion which can be obtained as respectively:

$$U_g = \omega_g \left(\frac{d_g}{2} \sin \alpha + y \right) \tag{5}$$

$$U_p = \omega_p \left(\frac{d_p}{2} \sin \alpha + y \right) \tag{6}$$

where ω is the angular velocity; d is the pitch diameter; α is the pressure angle; y is the distance from the pitch point to the instantaneous point.

3

2.4 Archard's wear model

In this study, the Archard's wear equation was employed to determine the tooth wear process in a spur gear system.

$$\frac{V}{s} = K\frac{W}{H} \tag{7}$$

where, V represents the volume of worn material, s represents the relative sliding distance between mating surfaces, K represents the dimensionless wear coefficient, W represents the load on the mating surfaces, H represents the hardness of mating material.

As mentioned earlier, the sliding distance varies with the motion of the meshing point on the line of action. So, it is critical important to investigate the wear on each local point rather than during contact. If wear is described as any point 'p' on the meshing surface, the Archard's wear equation can be written as follows:

$$h_p = \int_0^s kpds \tag{8}$$

where, h_p is the wear depth of point 'p'; k is the dimensional wear coefficient; p is the local contact pressure which can be obtained from Eq (2). After n revolution, the accumulated wear depth is:

$$h_{p,(n)} = h_{p,(n-1)} + kP_{p,(n-1)}S_p \tag{9}$$

where, $h_{p,(n)}$ is the wear depth at point 'p' on the tooth surface after n revolution, $h_{p,(n-1)}$ is the wear depth at the same contact point but one revolution before, $P_{p,(n-1)}$ is the pressure on point 'p'.

By substituting the sliding distance S_p derived from the previous Eq (3) and (4) into the Eq (9), the accumulated gear tooth wear can be estimated.
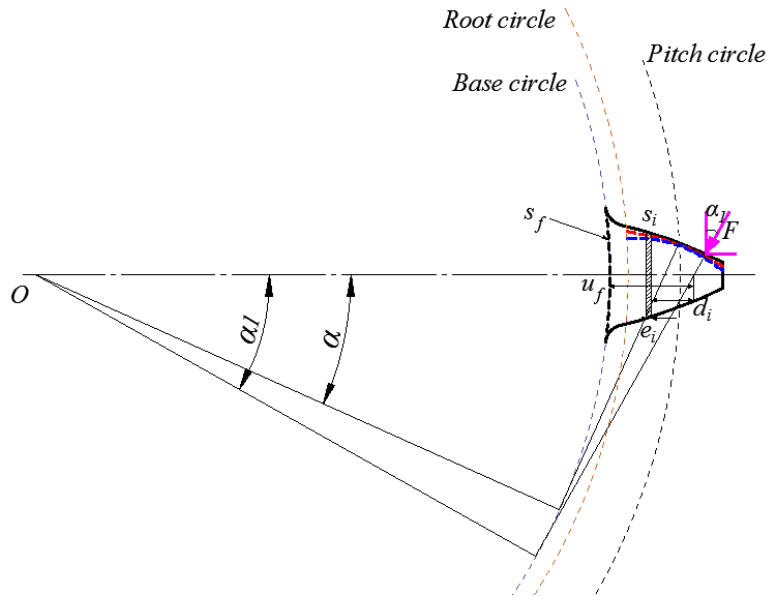

Figure 3 Modelling spur gear tooth as a non-uniform cantilever beam with tooth wear.

3 Gear mesh stiffness calculation

Gear mesh stiffness is a very important parameter which can reflect the gear mesh conditions. Normally, the gear mesh stiffness varies with the change in mesh tooth pair, the deviation of gear tooth profile, and the variation of installed centre distance. Considering the gear wear is a progressive removal of the surface material along gear tooth profile which could result in the variation of gear mesh stiffness, and further deteriorate the

4

gear dynamics. In this study, the gear mesh stiffness was calculated based on the potential energy method referenced by [11]. The stiffness of one mesh tooth is calculated from the bending deflections, fillet-foundation deflections and contact deflection. The detailed calculation was shown as follows.

3.1 Involute gear profile

According to the generation principle of the involute gear profile, the equation of gear profile can be estimated by the following equation.

$$
\begin{cases}
x_d = r_b(\sin\alpha - \alpha\cos\alpha) \\
y_d = r_b(\cos\alpha + \alpha\sin\alpha)
\end{cases}
\tag{10}
$$

The updated involute gear profile can be obtained by substituting the wear depth into the equation of the involute gear profile:

$$
\begin{cases}
x_{d1} = r_b(\sin\alpha - \alpha\cos\alpha) - h_{p,n}\sin\alpha_1 \\
y_{d1} = r_b(\cos\alpha + \alpha\sin\alpha) - h_{p,n}\cos\alpha_1
\end{cases}
\tag{11}
$$

Furthermore, the mesh stiffness can be estimated by integrating the updated toot profile into the following sections.

3.2 Bending deflection

The gear tooth can be regarded as a non-uniform cantilever beam with the length *L* which was divided into n segments as shown in Figure 3.The bending deflection of a tooth can be calculated in an expression as:

$$
\delta_b = F\cos^2\alpha_m \sum_{i=1}^{n} e_i \left\{ \frac{(d_i - e_i d_i + \frac{1}{3}e_i^2)}{E'\bar{I}_i} + \frac{1}{s_n G\bar{A}_i} + \frac{\tan^2\alpha_m}{\bar{A}_i E'} \right\}
\tag{12}
$$

where *F* is the applied force, α_m is the operating pressure angle, *G* is the shear modulus, S_n is a shear factor, e_i and d_i are given in Figure 3. *E'*, I_i and A_i are expressed as:

$$
E' = \frac{E(1-v)}{(1+v)(1-2v)}
$$

$$
\frac{1}{\bar{I}_i} = \left(\frac{1}{I_i} + \frac{1}{I_{i+1}}\right)/2
$$

$$
\frac{1}{\bar{A}_i} = \left(\frac{1}{A_i} + \frac{1}{A_{i+1}}\right)/2
$$

where, I_i and A_i are the inertia moment and the area of the tooth cross section S_i, *E* is the Young modulus and v is the Poisson's ratio.

The corresponding bending stiffness of the tooth can be obtained by:

$$
k_b = \frac{F}{\delta_b}
\tag{13}
$$

3.3 Fillet-foundation deflections

The analytical expression of calculating fillet-foundation deflection is given by:

$$\delta_f = \frac{F \cos^2 \alpha_m}{WE} \left\{ L^* \left(\frac{u_f}{S_f} \right)^2 + M^* \left(\frac{u_f}{S_f} \right) + P^*(1 + Q^* \tan^2 \alpha_m) \right\} \qquad (14)$$

where, W is the tooth width, u_f and S_f are given in Figure 3. The coefficients L^*, M^*, P^*, Q^* can be approached by referencing the polynomial function put forward by Sainsot [12].

The corresponding fillet-foundation stiffness can be obtained by:

$$k_f = \frac{F}{\delta_f} \qquad (15)$$

3.4 Contact deflection

According to the results derived by [13], the stiffness of the Hertzian contact of the two meshing teeth is a constant along the line of action. k_h can be given by:

$$k_h = \frac{\pi E W}{4(1 - v)} \qquad (16)$$

The local deformation is then expressed by:

$$\delta_h = \frac{F}{k_h} \qquad (17)$$

3.5 Total gear mesh stiffness

For a gear pair in contact, the total mesh stiffness K_{12} can be obtained as:

$$K_{12} = \frac{1}{k_{bg} + k_{fg} + k_{bg} + k_{bp} + k_h} \qquad (18)$$

Parameters	Symbol	Value
Tooth number	z_g/z_p	58/47
Module (mm)	m	1.4
Face width (mm)	b	25
Pressure angle (°)	α	20
Centre distance (mm)	a	74
Young's modulus ()	E	200GPa
Poisson's ratio	v	0.28
Wear coefficient	k	1×10^{-16} m^2/N

Table 1 Main parameters of the modelled gear set

4 Modelling results

4.1 Wear depth

In order to verify the model, a pair of spur gear was chosen to conduct the simulations, the main parameters of the gears geometry was depicted in Table 1 As shown in Figure 4 (a), the maximum Hertzian pressure at the meshing point decreases first then increases gradually after the meshing point passes through the pitch point. Due to the variation in mesh tooth pair, there is a sharp change of the Hertzian pressure when the mesh tooth pair changes from two to one or from one to two. Figure 4(a) also illustrates the change of Hertzian pressure under different loads. With the increase of the operating loads, the maximum Hertzian pressure increase correspondingly as the Hertzian equation shows the contact pressure is proportional to the operating

force. Figure 4 (b) shows the sliding distance of the driving gear which decreases gradually first, then increases after passing through the pitch point. As can be observed from the figure, there is no sliding motion only rolling motion between the mating gears at the pitch point. Besides, the sliding distance become bigger with the increase of the operating load.
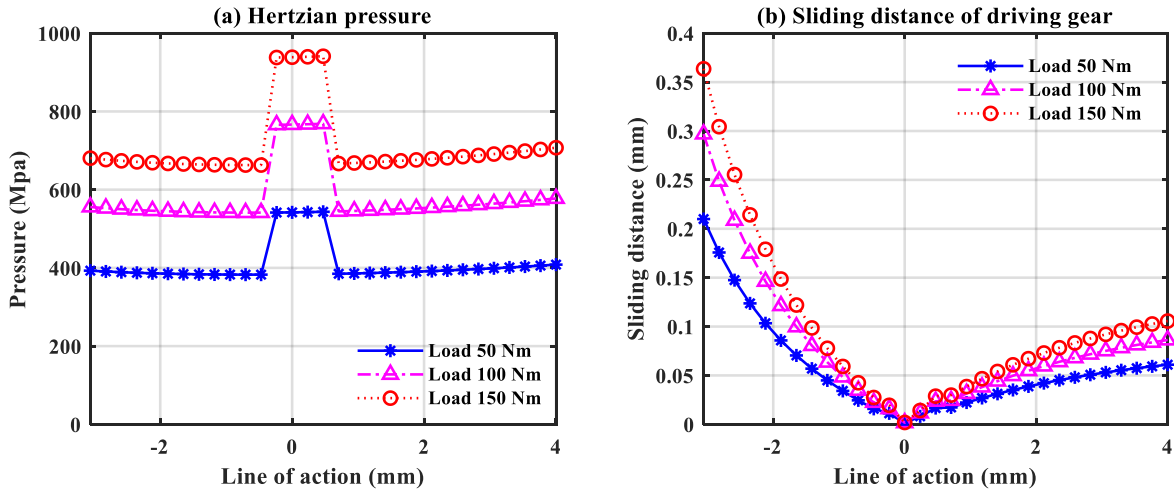

Figure 4 The maximum Hertzian pressure after 1×10^4 revolutions under different loads.

As depicted in the previous section, the wear depth is mainly affected by the contact pressure and sliding distance. As can be observed in Figure 5 (a), at the beginning of the mesh process, the wear depth decreases under the combined effect of the relative sliding motion and contact pressure. There is a sharp change in wear depth due to the sudden change in contact pressure induced by the variation of the mesh tooth pair. When the meshing point passes through the pitch point, the wear depth increases along the line of action. This variation is consistent with the changing trend of the sliding motion. Figure 5 also illustrates that the most severe worn place along the gear tooth face is near the tooth tip both for gear and pinion due to the sliding motion. Figure 5 (b) shows the change in wear depth under different operating revolutions which has the same changing tendency as the change with operating load. With the increase of the operating revolutions, the accumulated gear tooth wear increases.
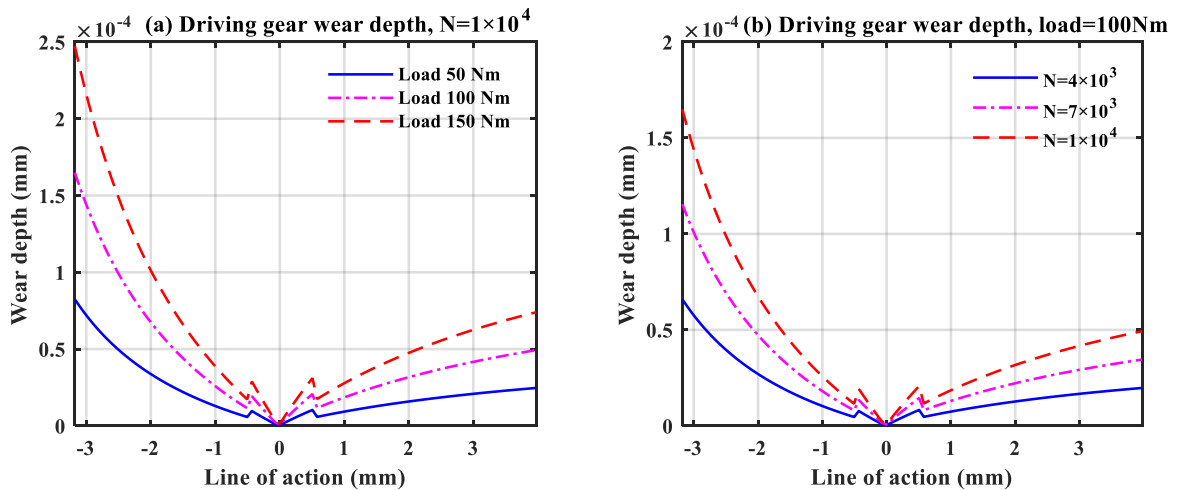

Figure 5 The wear depth of the gear and pinion after 1×10^4 revolutions under different loads

4.2　Time-varying mesh stiffness with surface wear

According to Sections 2 and 3, the wear depth and time-varying mesh stiffness can be evaluated respectively. In fact, the gear tooth wear alters the involute gear profile, which leads to the change in the geometric parameters e_i, I_i and A_i, correspondingly, thus the bending stiffness will be affected.

7

Figure 6 (a) illustrates the change in time-varying mesh stiffness with both the gear and pinion got worn after 1×10^4 revolutions. When the load increases, the gear tooth wear depth increases which leads to the reduction of gear mesh stiffness. Moreover, the reduction in gear mesh stiffness on the double-tooth-meshing area is more severe than on the single-tooth-pair meshing area. Figure 6(b) shows the gear mesh stiffness under different operating revolutions. The wear depth increase with the increase of operating revolutions, further resulting in a reduction on gear mesh stiffness. Theoretically, the reason is that the wear reduces the tooth thickness, resulting in the reduction of the potential energy. Thus, the gear tooth stiffness decreases.
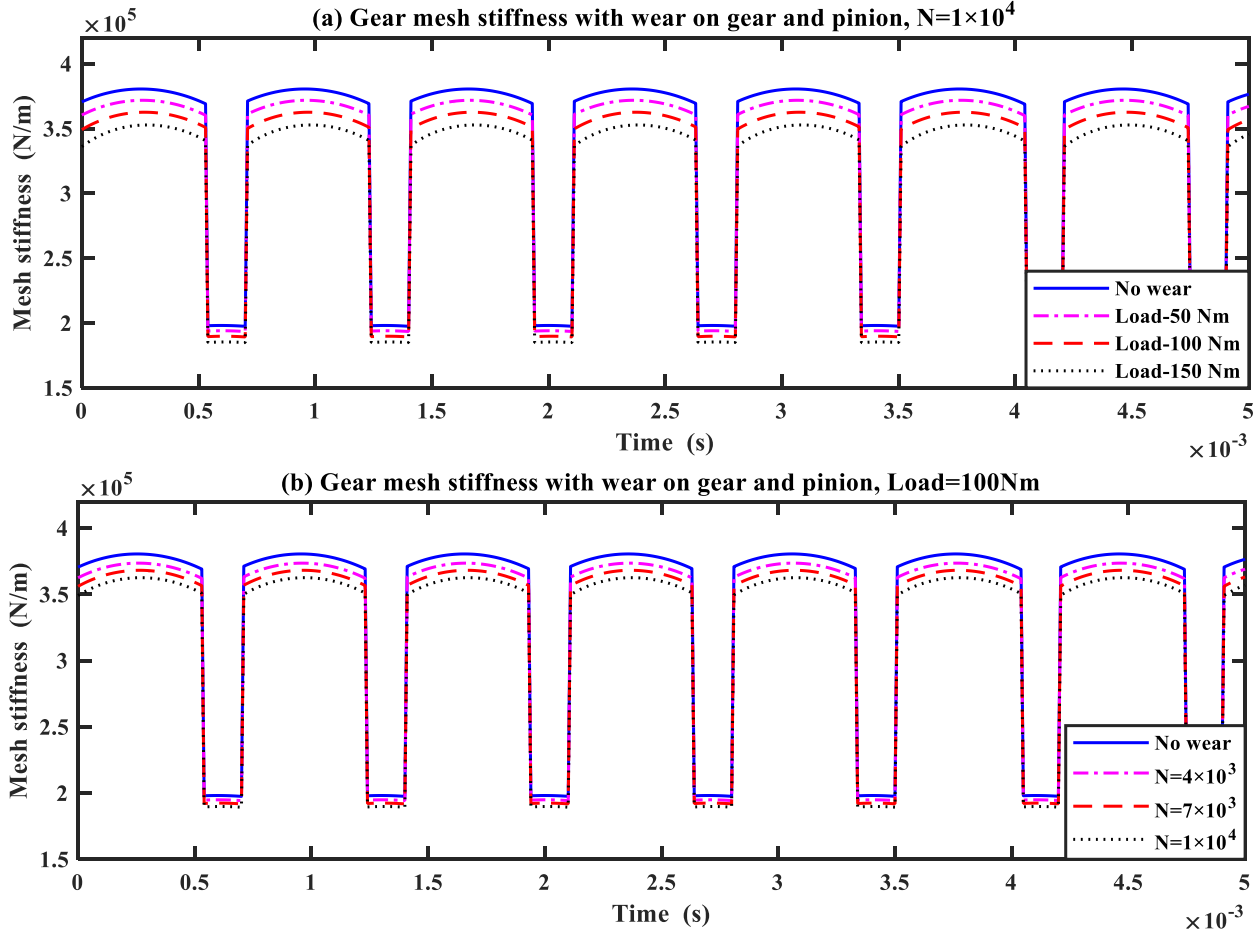

Figure 6 Gear mesh stiffness with wear progression on both gear and pinion

Figure 7 depicts the variation in gear mesh stiffness with driving gear wear only. As can be observed in Figure 7 (a), the mesh stiffness decrease with the increase of the wear depth due to the incremental operating load. On the condition of wear only existed on the driving gear, the mesh stiffness shows a downward trend in every mesh cycle. Figure 7 (b) shows the change in mesh stiffness under different revolutions, which gives the same indication that the wear will result in a reduction on gear mesh stiffness.

4.3   Verification of the simulation results

In order to verify the reliability of the results obtained, a literature review relating to the studies of correlation between the gear wear and gear dynamics were carried out. Some relative studies were found which have the similar results as illustrated in this study. In T.Osman's study [14], the gear tooth wear will reduce the dynamic response which can be beneficial in terms of vibration to a certain extent. Liu [15] investigate the coupling effect between surface wear and dynamics in a spur gear system, the results show that the equivalent gear mesh stiffness decrease with the increase of the wear depth. Thus, through the review of the relative studies, the model proposed in this study is proved to be reliable and meaningful.

5 Conclusion

In this study, a modified numerical model was proposed to evaluate the influence of gear tooth wear on time-varying mesh stiffness theoretically. The model was testified under different operating loads and operating revolutions. The results of the wear prediction illustrates that the gear tooth wear depth decreases firstly then increase gradually due to the combined effect of sliding and rolling motion. The increase in operating load will lead to high contact pressure between the mating gears, then accelerate the tooth wear process. Moreover, the gear tooth wear will cause the deviation in the tooth profile and tooth thickness. The modified TVMS model depicts that the different wear severities will cause the reduction in gear mesh stiffness. With wear both on the gear and pinion, the TVMS has an overall decrease when the wear depth accumulated. However, the TVMS will decline to one side when only one gear got worn. In addition, the reduction in mesh stiffness on the double-tooth-meshing area are much more obvious than that on the single-tooth-meshing area.

The proposed model, which is used for the TVMS prediction, can be integrated into the dynamic simulation of the spur gear transmission system. By doing this, the dynamic effect induced by gear tooth wear can be estimated.
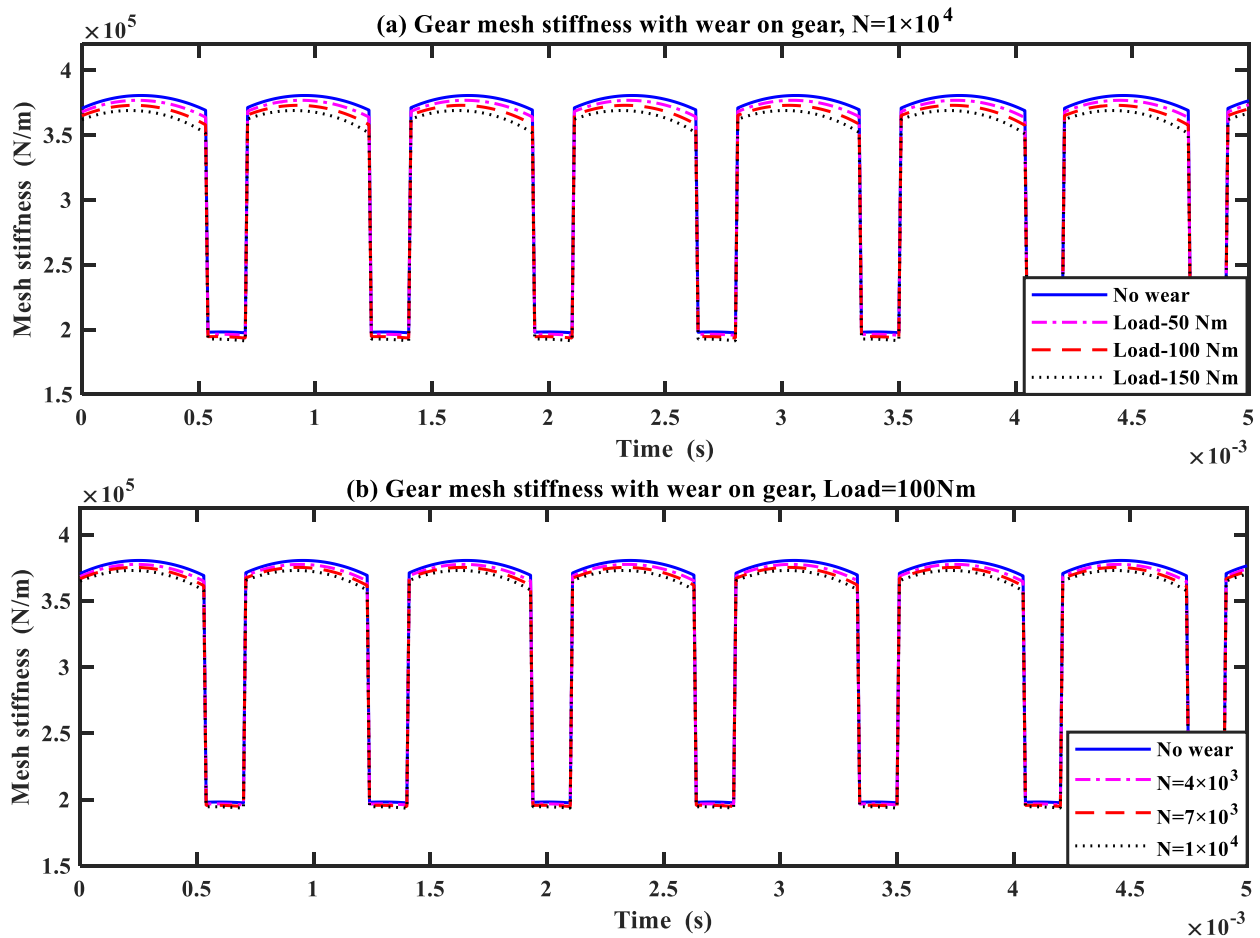

Figure 7 Gear mesh stiffness with wear progression on driving gear

6 Acknowledgments

7 References

[1] A. Flodin and S. Andersson, "Simulation of mild wear in spur gears," *Wear*, vol. 207, no. 1, pp. 16–23, Jun. 1997.

[2] P. Põdra and S. Andersson, "Wear simulation with the Winkler surface model," *Wear*, vol. 207, no. 1, pp. 79–85, Jun. 1997.

[3] A. Flodin and S. Andersson, "Simulation of mild wear in helical gears," *Wear*, vol. 241, no. 2, pp. 123–128, Jul. 2000.

[4] A. Flodin and S. Andersson, "A simplified model for wear prediction in helical gears," *Wear*, vol. 249, no. 3, pp. 285–292, May 2001.

[5] A. Kahraman, P. Bajpai, and N. E. Anderson, "Influence of Tooth Profile Deviations on Helical Gear Wear," *J. Mech. Des.*, vol. 127, no. 4, p. 656, 2005.

[6] M. Ş. Tunalioğlu and B. Tuç, "Theoretical and experimental investigation of wear in internal gears," *Wear*, vol. 309, no. 1, pp. 208–215, Jan. 2014.

[7] V. Onishchenko, "Investigation of tooth wears from scuffing of heavy duty machine spur gears," *Mech. Mach. Theory*, vol. 83, pp. 38–55, Jan. 2015.

[8] F. Zhao, Z. Tian, X. Liang, and M. Xie, "An Integrated Prognostics Method for Failure Time Prediction of Gears Subject to the Surface Wear Failure Mode," *IEEE Trans. Reliab.*, vol. 67, no. 1, pp. 316–327, Mar. 2018.

[9] M. Stanković, A. Marinković, A. Grbović, Ž. Mišković, B. Rosić, and R. Mitrović, "Determination of Archard's wear coefficient and wear simulation of sliding bearings," *Ind. Lubr. Tribol.*, vol. 71, no. 1, pp. 119–125, Jan. 2019.

[10] A. Shebani and C. Pislaru, "Wear Measuring and Wear Modelling Based on Archard, ASTM, and Neural Network Models," *Int. J. Mech. Aerosp. Ind. Mechatron. Eng.*, vol. 9, pp. 177–182, Jan. 2015.

[11] F. Chaari, T. Fakhfakh, and M. Haddar, "Analytical modelling of spur gear tooth crack and influence on gearmesh stiffness," *Eur. J. Mech. - ASolids*, vol. 28, no. 3, pp. 461–468, May 2009.

[12] P. Sainsot, P. Velex, and O. Duverger, "Contribution of Gear Body to Tooth Deflections—A New Bidimensional Analytical Formula," *J. Mech. Des.*, vol. 126, no. 4, pp. 748–752, Aug. 2004.

[13] D. C. H. Yang and Z. S. Sun, "A Rotary Model for Spur Gear Dynamics," *J. Mech. Transm. Autom. Des.*, vol. 107, no. 4, pp. 529–535, Dec. 1985.

[14] T. Osman and Ph. Velex, "Static and dynamic simulations of mild abrasive wear in wide-faced solid spur and helical gears," *Mech. Mach. Theory*, vol. 45, no. 6, pp. 911–924, Jun. 2010.

[15] X. Liu, Y. Yang, and J. Zhang, "Investigation on coupling effects between surface wear and dynamics in a spur gear system," *Tribol. Int.*, vol. 101, pp. 383–394, Sep. 2016.